Fibroblast activation protein targeted PET/CT with ^{68}Ga-FAPI for imaging IgG4-related disease: comparison to ^{18}F-FDG PET/CT

[1,2]Yaping Luo, [1,2]Qingqing Pan, [3]Huaxia Yang, [3]Linyi Peng, [3]Wen Zhang, [1,2]Fang Li†

[1]Department of Nuclear Medicine, [3]Department of Rheumatology

Chinese Academy of Medical Sciences and Peking Union Medical College Hospital;

[2]Beijing Key Laboratory of Molecular Targeted Diagnosis and Therapy in Nuclear Medicine

†Corresponding Author:

Fang Li

Department of Nuclear Medicine

Chinese Academy of Medical Sciences and Peking Union Medical College Hospital;

Beijing Key Laboratory of Molecular Targeted Diagnosis and Therapy in Nuclear Medicine

Wangfujing, Dongcheng District, Beijing 100730, P.R. China

Email: lifang@pumch.cn

Telephone: 86-10-69155502

First Author:

Yaping Luo

Department of Nuclear Medicine

Chinese Academy of Medical Sciences and Peking Union Medical College Hospital

Wangfujing, Dongcheng District, Beijing 100730, P.R. China

Email: luoyaping@live.com

Telephone: 86-10-69155513

Word Count: 4461

Running title: ^{68}Ga-FAPI PET/CT in IgG4-RD

ABSTRACT

IgG4-related disease (IgG4-RD) is characterized by lymphoplasmacytic infiltration

enriched in IgG4-positive plasma cells and variable degrees of fibrosis with a

characteristic storiform pattern. Since fibrosis is an important feature of IgG4-RD, we

performed a prospective cohort study to evaluate the performance of ^{68}Ga-FAPI, a

recently introduced PET agent targeting fibroblast activation protein, in IgG4-RD.

Methods: Twenty-six patients with IgG4-RD were recruited. All patients underwent both

^{68}Ga-FAPI and ^{18}F-FDG PET/CT. The positive rates of the PET/CT scans in the involved

organs and the uptake values were compared. **Results:** In a total of 136 organ

involvements in the 26 patients, ^{68}Ga-FAPI PET/CT additionally detected 18/136 (13.2%)

organ involvements in 13/26 (50.0%) patients compared with ^{18}F-FDG PET/CT.

^{68}Ga-FAPI PET/CT had a higher positive rate than ^{18}F-FDG PET/CT in detecting

involvement in the pancreas, bile duct/liver, and lacrimal gland. ^{68}Ga-FAPI also

demonstrated significantly higher uptake than ^{18}F-FDG in the matched disease in the

pancreas, bile duct/liver, and salivary gland ($p < 0.01$). However, lymph node

involvements with flip-flop uptake of ^{18}F-FDG were not accumulating ^{68}Ga-FAPI.

Conclusions: ^{68}Ga-FAPI might be a promising imaging agent for the assessment of

IgG4-RD.

KEY WORDS:

IgG4-related disease, fibroblast activation protein, ^{68}Ga-FAPI, PET/CT

INTRODUCTION

IgG4-related disease (IgG4-RD) is an autoimmune-mediated disorder associated with a

diffuse mass-forming inflammatory reaction. It can affect nearly any anatomic site and

may be confused with malignancy, infection or other immune-mediated disease (*1,2*).

Although IgG4-RD could affect any organ, there are predilections for certain organ

involvements with a synchronous or metachronous pattern, including salivary gland,

orbits and lacrimal gland, pancreas, biliary tree, lung, kidney, aorta and retroperitoneum,

and thyroid gland (*1-3*). The diagnosis of IgG4-RD often requires the integration of

clinical, serological, radiological, pathological, and immunohistological features (*3*). The

3 central histopathological features of IgG4-RD are lymphoplasmacytic infiltration

enriched in IgG4-positive plasma cells, obliterative phlebitis, and stroriform fibrosis (*4-6*).

Sometimes even with supporting histopathological evidence, clinicopathological

correlation is needed to confirm the diagnosis of IgG4-RD, and imaging is an important

aspect of the diagnostic workup.

^{18}F-FDG PET can help to detect the extent of organ involvement and to monitor

disease activity after treatment in IgG4-RD (*1*). In a retrospective study on ^{18}F-FDG

3

PET/CT for differential diagnosis of patients with clinically suspected IgG4-RD,

^{18}F-FDG PET/CT had a sensitivity of 85.7% and specificity of 66.1% for diagnosing

IgG4-RD, mainly based on the SUVmax of main involved organ, SUVmax of

submandibular glands, and the presence of multi-organ involvement (*7*). However,

consistent with the false-negative results of ^{18}F-FDG PET noted in some studies (*7,8*), we

also encountered cases of IgG4-RD that displayed only mild or normal FDG uptake in the

involved organs in our clinical practice. In the above-mentioned retrospective study, the

FDG uptake in the major involved organs displayed a mean SUVmax of 4.6 ± 1.7, with a

relatively wide range from 1.1 to 7.8 (*7*). The low-grade FDG uptake in these cases may

partly limit the utility of ^{18}F-FDG PET in differential diagnosis, staging, and evaluation

of treatment response in IgG4-RD.

Recently, ^{68}Ga-FAPI that targets fibroblast activation protein (FAP) is introduced in

tumor imaging, as FAP is highly expressed in cancer-associated fibroblasts in the stroma

of several tumor entities (*9,10*). In addition to solid tumors, FAP was also shown to be

expressed in rheumatoid arthritis, artherosclerotic plaques, fibrosis and ischemic heart

4

tissue after myocardial infarction (*9,10*). Preclinical studies of immuno-PET and immuno-SPECT with radiolabeled anti-FAP antibody showed high tracer accumulation in the inflamed joints that correlated with the severity of the inflammation in murine experimental rheumatoid arthritis (*11-13*). In IgG4-RD, fibrosis arising from the extracellular matrix component produced by the large number of fibroblasts is a major histopathological feature (*1,6*); thus we speculate that it is possible for IgG4-RD to be imaged with ^{68}Ga-FAPI. We recently reported 2 cases of IgG4-RD showing intense ^{68}Ga-FAPI uptake in the involved organs (*14,15*). In the present study, we aimed to further evaluate the performance of ^{68}Ga-FAPI PET/CT in IgG4-RD and to compare it with the performance of ^{18}F-FDG PET/CT, which served as a reference.

PATIENTS AND METHODS

Study Design and Patients

This is a preliminary report of an ongoing prospective study evaluating the role of ^{68}Ga-FAPI PET/CT in the management of IgG4-RD. The study was approved by the institutional review board of Peking Union Medical College Hospital (protocol #ZS-1810)

and registered at Clinicaltrial.gov (NCT 04125511). A total of 26 patients diagnosed with

IgG4-RD in the Department of Rheumatology of the Peking Union Medical College

Hospital were consecutively recruited from Feb 2019 to January 2020. Written informed

consent was obtained from each patient. All recruited patients fulfilled the 2019

American College of Rheumatology/European League Against Rheumatism classification

criteria for IgG4-RD (*3*). After enrollment, patients were referred for ^{18}F-FDG and

^{68}Ga-FAPI PET/CT for evaluation of the disease, which were carried out within 1 week.

The imaging characteristics were analyzed afterwards.

PET/CT Imaging

The radiolabeling of ^{68}Ga-FAPI was performed manually immediately before injection.

Briefly, 92 μL sodium acetate (1.25 M) was added to 1 mL ^{68}GaCl$_3$ eluent (^{68}Ga^{3+} in 1.0

M HCl) obtained from a ^{68}Ge/^{68}Ga generator (ITG, Germany) to adjust the pH to 3.5-4.0.

After the addition of an aliquot of 20 μl (1 μg/μl) FAPI-04 (CSBio Co, CA94025, USA),

the mixture was heated to 100 °C for 10 min. The reaction solution was diluted to 5 ml

and passed through a preconditioned Sep-Pak C18 Plus Light cartridge (Waters, USA),

and the cartridge was eluted with 0.5 ml 75% ethanol to obtain the final product. The

radiochemical purity of the product was analyzed by thin-layer chromatography. The

^{68}Ga-FAPI injections were filtered through a 0.22 μm Millex-LG filter (EMD Millipore)

before clinical use.

^{18}F-FDG was synthesized in-house with an 11 MeV cyclotron (CTI RDS 111, Siemens,

Germany).

The PET scans were performed on dedicated PET/CT scanners (Biograph 64

Truepoint TrueV, Siemens, Germany; Polestar m660, SinoUnion, China). Two patients

underwent ^{18}F-FDG PET/CT at outside hospitals. For ^{18}F-FDG PET/CT, the patients

fasted for over 6 h, and the blood glucose levels were monitored (4.5-8.8 mmol/L) prior

to an injection of ^{18}F-FDG (5.55 MBq/kg). The PET/CT images (2 min/bed) were

acquired with an uptake time of 68.5 ± 12.1 min (range 47-90 min). For ^{68}Ga-FAPI

PET/CT, imaging was performed (2-3 min/bed) with an uptake time of 54.4 ± 15.8 min

(range 40-80 min) after an injection of 85.2 ± 27.0 MBq (range 55.5-162.8 MBq)

^{68}Ga-FAPI. The emission scan was obtained from the tip of the skull to the mid-thigh. All

patients underwent unenhanced low-dose CT (120 kV, 30-50 mAs) for attenuation

correction and anatomical reference. The acquired data were reconstructed using the

ordered-subset expectation maximization method (Siemens Biograph 64: 2 iterations, 8

subsets, Gaussian filter, FWHM 5 mm, image size 168*168; SinoUnion Polestar: 2

iterations, 10 subsets, Gaussian filter, FWHM 4 mm, image size 192*192).

Image Interpretation and Statistical Analysis

The PET/CT images were transferred to a Siemens MMWP workstation. Two

experienced nuclear medicine physicians (YL and QP) visually assessed the PET/CT

images and were in consensus for the image interpretation of organ involvements. The

presence and sites of IgG4-RD involvements, and the intensity of the uptake in the

lesions were recorded. Increased radioactivity compared with the background uptake was

defined as being positive. The SUV of the lesions were measured by the same nuclear

medicine physician (YL) using the volume of interest method with a unified standard.

The McNemar test was used to statistically compare the positive rates of ^{68}Ga-FAPI and

^{18}F-FDG PET/CT in detecting organ involvements of IgG4-RD. The differences of

8

SUVmax between ^{68}Ga-FAPI and ^{18}F-FDG PET/CT was performed using paired Student

t-test. A p-value <0.05 was considered statistically significant.

RESULTS

Clinical Characteristics

Twenty-six patients with IgG4-RD (20 men and 6 women; 51.5 ± 12.9 yr, range 17-64

yr) were enrolled in the present study. Nineteen patients had newly diagnosed IgG4-RD

that was treatment-naïve; 7 patients had a previous history of IgG4-RD and had been

treated with prednisone or other medication, but had recurrent or persistent disease at

enrollment. The median level of serum IgG4 was 14500 (range, 355-73400) mg/L

(normal limits 80-1400 mg/L). Seventeen patients (65.4%) underwent biopsy for

diagnosis of IgG4-RD (biopsy site: pancreas [n=7], salivary gland [n=4], lacrimal gland

[n=2], lymph node [n=2], lung [n=2], retroperitoneal mass [n=1], kidney [n=1], gall

bladder [n=1]).

In the recruited patients, IgG4-RD most commonly involved the pancreas (19/26,

73.1%), salivary gland (19/26, 73.1% [submandibular gland, 19/26, 73.1%; parotid, 7/26,

9

26.9%; sublingual gland, 7/26, 26.9%]), lymph nodes (16/26, 61.5%), and lacrimal gland

(14/26, 53.8%, extraocular muscle was also involved in one patient). Other involved

organs included lung (9/26, 34.6%), pleura (6/26, 23.1%), bile duct and liver (6/26,

23.1%, gall bladder was also involved in one patient), retroperitoneal fibrosis/periaortitis

(7/26, 26.9%), kidney (5/26, 19.2%), prostate (9/26, 34.6%), seminal vesicle (3/26,

11.5%), peritoneum (3/26, 11.5%), nasal cavity (3/26, 11.5%), and pituitary stalk (1/26,

3.8%). The clinical characteristics are summarized in Table 1.

Comparison of ^{68}Ga-FAPI and ^{18}F-FDG PET/CT

^{68}Ga-FAPI PET/CT were visually positive for detecting involvements of IgG4-RD in

26/26 (100%) patients, whereas ^{18}F-FDG PET/CT results were positive for 24/26 (92.3%)

patients. In a total of 136 organ involvements in the 26 patients, ^{68}Ga-FAPI PET/CT

additionally detected 18/136 (13.2%) organ involvements in 13/26 (50.0%) patients

compared with ^{18}F-FDG PET/CT (FAPI+/FDG-), including the disease in the pancreas

(8/19), lacrimal gland (4/14), sublingual gland (2/7), submandibular gland (1/19), bile

duct and liver (2/6), and nasal cavity (1/3). However, all of the lymph node involvements

10

that were FDG-avid were missed by ^{68}Ga-FAPI PET/CT (FAPI-/FDG+). False negative

organ involvement of both tracers (FAPI-/FDG-) were found in 2 patients: one patient

(patient#12) with IgG4-related lung disease who had been previously treated with

prednisone for 3 years, the lung disease did not show ^{18}F-FDG or ^{68}Ga-FAPI uptake in

PET (FAPI-/FDG-), but some patches in the lung were shown in the coregistered CT;

another patient (patient#19) with membranous glomerulonephritis was negative for the

kidney disease in both ^{18}F-FDG and ^{68}Ga-FAPI PET/CT. The remaining involvements

were interpreted as being positive with both tracers (FAPI+/FDG+). The detection rate of

^{68}Ga-FAPI and ^{18}F-FDG PET/CT in IgG4-RD involvements is shown in Table 2

(diagnostic performance of dual-tracer PET/CT in each case shown in supplement Table

1).

When visually comparing the uptake and the extension of organ involvements detected

in PET/CT, ^{68}Ga-FAPI showed much higher contrast or detected more extensive disease

in the pancreas, bile duct/liver, salivary gland than ^{18}F-FDG in more than 50% of the

recruited patients with the above involvements. For quantitative comparison, the

SUVmax of the matched disease in the pancreas, bile duct/liver, and salivary gland was

significantly higher in ^{68}Ga-FAPI PET/CT (pancreas, 15.22 ± 8.99; bile duct/liver, $9.42 \pm$

4.36; salivary gland, 8.26 ± 3.90) than in ^{18}F-FDG PET/CT (pancreas, 4.19 ± 2.52; bile

duct/liver, 4.58 ± 2.08; salivary gland, 4.88 ± 1.90) (paired Student t-test, $p < 0.01$).

Meanwhile, the lymph node involvements had significantly higher uptake in ^{18}F-FDG

PET/CT (SUVmax, 6.37 ± 1.72) than in ^{68}Ga-FAPI PET/CT (SUVmax, 1.61 ± 0.76) in

all patients with IgG4-related lymphadenopathy (paired Student t-test, $p < 0.0001$).

Comparing the uptake of ^{68}Ga-FAPI versus ^{18}F-FDG by involvements in lacrimal gland,

lung/pleura, periaortitis/retroperitoneal fibrosis, kidney, and prostate/seminal vesicle, the

average SUVmax presented no relevant differences ($p > 0.05$). The visual and

quantitative comparison of organ involvements of IgG4-RD between ^{68}Ga-FAPI and

^{18}F-FDG PET/CT are shown in Figure 1 and Table 3, respectively; and examples of

maximum intensity projections of the dual-tracer PET scans in IgG4-RD are shown in

Figure 2.

DISCUSSION

^{68}Ga-FAPI is a recently introduced pan-tumor PET agent targeting FAP, a type II transmembrane serine protease. Overexpression of FAP protein is a distinct feature of cancer-associated fibroblasts while not found in normal fibroblasts (*9,10*). In IgG4-RD, myofibroblasts and fibroblasts are activated by polarised CD4-positive T-cell population to drive fibrosis (*1*). Histopathologically, fibroblasts and myofibroblasts are intermingled with lymphoplasmacytic infiltrate and fibrosis, especially in the active phase of IgG4-RD (*2*). Although there is no direct evidence to confirm the overexpression of FAP in IgG4-RD, we speculate that the high accumulation of ^{68}Ga-FAPI in IgG4-RD results from the uptake by the activated fibroblasts or myofibroblasts.

In our study, we found high ^{68}Ga-FAPI uptake in the involved organs of IgG4-RD, especially in the pancreas, bile duct/liver, and salivary gland. In contrast, lymph node involvement was FAPI-negative. There are 5 histological patterns in IgG4-related lymphadenopathy, including multicentric Castleman disease-like, follicular hyperplasia, interfollicular expansion, progressive transformation of germinal center-like, and nodal inflammatory pseudotumor-like types. Fibrosis is not seen in most of the IgG4-related

13

lymphadenopathy except in inflammatory pseudotumor-like lesions (*6,16*). This fact

explains the false-negative results of ^{68}Ga-FAPI PET in lymph node involvements in our

study. Regarding the histopathological confirmation of IgG4-RD, the 3 major features are

dense lymphoplasmacytic infiltration, storiform fibrosis, and obliterative phlebitis. Note

that infiltration of IgG4-positive plasma cells may also be found in other diseases (eg.,

ANCA-associated disease, diabetic nephropathy, multicentric Castleman's disease,

rheumatoid arthritis, pancreatic cancers), the characteristic storiform fibrosis and

obliterative phlebitis are considered to be more specific findings in IgG4-RD, and fibrosis

is a histological prerequisite for the diagnosis (*6*). On this account, the histopathological

diagnosis of IgG4-RD through lymph node biopsy alone is difficult because fibrosis and

obliterative phlebitis are lacking (*1,3*). Unlike ^{18}F-FDG that accumulates in cancer cells

and active inflammatory lesions from an enhancement of glycolytic flux, the ^{68}Ga-FAPI

uptake is suggested to be associated with the degree of fibrosis, thus ^{68}Ga-FAPI PET may

be preferred to ^{18}F-FDG PET in providing an optimal site for biopsy to diagnose

IgG4-RD.

14

We found ^{68}Ga-FAPI was superior or at least equal to ^{18}F-FDG for detecting IgG4-RD in lacrimal gland, salivary gland, pancreas, and bile duct/liver in all recruited patients. As mild ^{18}F-FDG uptake of salivary glands is usually observed in PET/CT as a normal variant, meanwhile the intense uptake in extraocular muscles may sometimes mask the orbital disease (*17,18*), the low background uptake of ^{68}Ga-FAPI in the head and neck (*19,20*) makes it advantageous over ^{18}F-FDG in detecting IgG4-RD in these organs. Moreover, ^{68}Ga-FAPI has favorable dosimetry profile and tracer kinetics for PET/CT imaging (*21*).

IgG4-RD was initially recognized in the pancreas (*6*), and it is also the most commonly affected organ in our study. For imaging diagnosis with PET/CT, diffusely enlarged pancreas with moderate to intense ^{18}F-FDG uptake without pancreaticobiliary duct obstruction is an important sign with strong confidence to indicate IgG4-RD (*22*). However, focal lesion in the pancreas with patchy ^{18}F-FDG uptake is less likely to indicate IgG4-RD and did not allow differentiation from pancreatic tumors (*7*). In our study, the pancreatic disease in 2 patients were depicted as focal lesions in the head of the

pancreas in ^{18}F-FDG PET/CT, but ^{68}Ga-FAPI PET/CT obviously showed diffuse

pancreatic disease with intense radioactivity in these 2 individuals (Figure 2, patient #13,

18). This finding enhanced the confidence for indicating IgG4-RD when interpreting the

images. However, diffusely increased ^{68}Ga-FAPI uptake in the pancreas should also be

differentiated with pancreatic cancer with tumor-induced pancreatitis (23). In another 8

patients, ^{68}Ga-FAPI PET/CT additionally detected the pancreatic disease that was not

FDG-avid, thus improving the detectability of IgG4-RD in the pancreas (^{68}Ga-FAPI vs.

^{18}F-FDG, 100% vs. 57.9%, $p < 0.01$). Similarly, ^{68}Ga-FAPI PET/CT has a higher

detection rate of involvements in the bile duct/liver than ^{68}Ga-FAPI PET/CT did,

although not statistically significant probably due to the limited sample size (^{68}Ga-FAPI

vs. ^{18}F-FDG, 100% vs. 66.7%, $p > 0.05$).

Few cases with involvements in the prostate, aorta, and lung presented visually lower

uptake of ^{68}Ga-FAPI than the uptake of ^{18}F-FDG in these anatomical sites. We think it is

probably due to the higher positron range and inferior image quality of ^{68}Ga, thus

delineation of some small lesions (eg., periaortitis in patient #4 that was less than 1 cm in

16

size) and prostatic disease adjacent to the bladder may be hampered with ^{68}Ga-FAPI

when comparing to ^{18}F-FDG. It is to be noted that prostate cancer also have moderate to

intense uptake of ^{68}Ga-FAPI (*19,24,25*), therefore IgG4-related prostatitis must be

differentiated from prostate cancer in elderly patients.

Glucocorticoid therapy is the first-line, standard-of-care approach for most patients

with IgG4-RD. A good and rapid response to glucocorticoids is a characteristic feature of

IgG4-RD (*1*). ^{18}F-FDG PET/CT results before and after treatment showed a good

correlation with treatment response in most cases of IgG4-RD (*8,22*). As for ^{68}Ga-FAPI,

we previously reported a case of IgG4-RD showing marked improvement of the lesions

detected in ^{68}Ga-FAPI PET/CT at baseline after treatment with prednisone and

cyclophosphamide for 2 months (*14*). The value of ^{68}Ga-FAPI in treatment response

monitoring needs to be further investigated.

Our study has several limitations. First, some recruited patients did not have

histopathological confirmation of IgG4-RD. Although biopsies are essential in many

settings to establish the diagnosis of IgG4-RD and exclude mimickers, the 2019

17

American College of Rheumatology/European League Against Rheumatism classification

criteria for IgG4-RD emphasized that biopsy is not required when the diagnosis of

IgG4-RD is straightforward on the basis of clinical, serological and radiological findings

(*3*). Such criteria are compatible with clinical practice and essential to the appropriate

diagnosis of patients in both clinical and research settings. Second, immunohistochemical

staining of FAP was not performed in our study. Previous studies have determined that

^{68}Ga-FAPI was bound with high specificity and selectivity to FAP-positive tumor cells

(*9,10*), we think the uptake of ^{68}Ga-FAPI in IgG4-RD may share the same mechanism,

however, further studies are warranted. Third, the heterogeneity of PET/CT protocols (eg.

uptake time, dose, use of 2 different PET/CT scanners and reconstruction parameters) in

our study may bias the SUV measurements.

CONCLUSION

In the present study, we found that ^{68}Ga-FAPI PET/CT had a higher detection rate or

higher uptake than ^{18}F-FDG did in IgG4-RD in most of the involved organs, especially in

the pancreas, bile duct/liver, lacrimal gland, and salivary gland. However, IgG4-related

18

lymphadenopathy was not FAPI-avid, which may be attributed to the fact that

IgG4-related lymphadenopathy usually lacks the characteristic storiform fibrosis. Further

studies are warranted to clarify the role of ^{68}Ga-FAPI in monitoring IgG4-RD.

DISCLOSURE:

KEY POINTS:

QUESTION: Is ^{68}Ga-FAPI PET/CT superior to ^{18}F-FDG PET/CT in detecting organ

involvement in IgG4-RD?

PERTINENT FINDINGS: In our prospective cohort study of 26 patients with IgG4-RD,

^{68}Ga-FAPI PET/CT showed a higher detection rate or higher uptake than ^{18}F-FDG did in

most of the involved organs, except the lymph node involvements.

IMPLICATIONS FOR PATIENT CARE: ^{68}Ga-FAPI PET/CT might be a promising tool

in the assessment of IgG4-RD.

REFERENCES

1. Kamisawa T, Zen Y, Pillai S, Stone JH. IgG4-related disease. *Lancet.*
2015;385:1460-1471.

2. Kubo K, Yamamoto K. IgG4-related disease. *Int J Rheum Dis.* 2016;19:747-762.

3. Wallace ZS, Naden RP, Chari S, et al. The 2019 American College of
Rheumatology/European League Against Rheumatism classification criteria for
IgG4-related disease. *Ann Rheum Dis.* 2020;79:77-87.

4. Cheuk W, Chan JK. IgG4-related sclerosing disease: a critical appraisal of an
evolving clinicopathologic entity. *Adv Anat Pathol.* 2010;17:303-332.

5. Smyrk TC. Pathological features of IgG4-related sclerosing disease. *Curr Opin
Rheumatol.* 2011;23:74-79.

6. Deshpande V, Zen Y, Chan JK, et al. Consensus statement on the pathology of
IgG4-related disease. *Mod Pathol.* 2012;25:1181-1192.

7. Lee J, Hyun SH, Kim S, et al. Utility of FDG PET/CT for differential diagnosis of
patients clinically suspected of IgG4-related disease. *Clin Nucl Med.* 2016;41:e237-243.

8. Ebbo M, Grados A, Guedj E, et al. Usefulness of

2-[18F]-fluoro-2-deoxy-D-glucose-positron emission tomography/computed tomography

for staging and evaluation of treatment response in IgG4-related disease: a retrospective

multicenter study. *Arthritis Care Res (Hoboken).* 2014;66:86-96.

9. Lindner T, Loktev A, Altmann A, et al. Development of quinoline-based theranostic

ligands for the targeting of fibroblast activation protein. *J Nucl Med.* 2018;59:1415-1422.

10. Loktev A, Lindner T, Mier W, et al. A tumor-imaging method targeting

cancer-associated fibroblasts. *J Nucl Med.* 2018;59:1423-1429.

11. Laverman P, van der Geest T, Terry SY, et al. Immuno-PET and immuno-SPECT of

rheumatoid arthritis with radiolabeled anti-fibroblast activation protein antibody

correlates with severity of arthritis. *J Nucl Med.* 2015;56:778-783.

12. Terry SY, Koenders MI, Franssen GM, et al. Monitoring therapy response of

experimental arthritis with radiolabeled tracers targeting fibroblasts, macrophages, or

integrin alphavbeta3. *J Nucl Med.* 2016;57:467-472.

13. van der Geest T, Laverman P, Gerrits D, et al. Liposomal treatment of experimental

arthritis can be monitored noninvasively with a radiolabeled anti-fibroblast activation

protein antibody. *J Nucl Med.* 2017;58:151-155.

14. Luo Y, Pan Q, Zhang W. IgG4-related disease revealed by (68)Ga-FAPI and

(18)F-FDG PET/CT. *Eur J Nucl Med Mol Imaging.* 2019;46:2625-2626.

15. Pan Q, Luo Y, Zhang W. Recurrent immunoglobulin G4-related disease shown on

^{18}F-FDG and ^{68}Ga-FAPI PET/CT. *Clin Nucl Med.* 2020;45:312-313.

16. Zen Y, Nakanuma Y. IgG4-related disease: a cross-sectional study of 114 cases. *Am J

Surg Pathol.* 2010;34:1812-1819.

17. Nakamoto Y, Tatsumi M, Hammoud D, Cohade C, Osman MM, Wahl RL. Normal

FDG distribution patterns in the head and neck: PET/CT evaluation. *Radiology.*

2005;234:879-885.

18. Basu S, Houseni M, Alavi A. Significance of incidental fluorodeoxyglucose uptake

in the parotid glands and its impact on patient management. *Nucl Med Commun.*

2008;29:367-373.

19. Giesel FL, Kratochwil C, Lindner T, et al. (68)Ga-FAPI PET/CT: biodistribution and

preliminary dosimetry estimate of 2 DOTA-containing FAP-Targeting agents in patients

with various cancers. *J Nucl Med.* 2019;60:386-392.

20. Loktev A, Lindner T, Burger EM, et al. Development of fibroblast activation

protein-targeted radiotracers with improved tumor retention. *J Nucl Med.*

2019;60:1421-1429.

21. Meyer C, Dahlbom M, Lindner T, et al. Radiation dosimetry and biodistribution of

(68)Ga-FAPI-46 PET imaging in cancer patients. *J Nucl Med*. 2019. [epub ahead of print]

22. Zhang J, Chen H, Ma Y, et al. Characterizing IgG4-related disease with (1)(8)F-FDG

PET/CT: a prospective cohort study. *Eur J Nucl Med Mol Imaging.* 2014;41:1624-1634.

23. Luo Y, Pan Q, Zhang W, Li F. Intense FAPI uptake in inflammation may mask the

tumor activity of pancreatic cancer in ^{68}Ga-FAPI PET/CT. *Clin Nucl Med.*

2020;45:310-311.

24. Kratochwil C, Flechsig P, Lindner T, et al. (68)Ga-FAPI PET/CT: tracer uptake in 28

different kinds of cancer. *J Nucl Med.* 2019;60:801-805.

25. Khreish F, Rosar F, Kratochwil C, Giesel FL, Haberkorn U, Ezziddin S. Positive

FAPI-PET/CT in a metastatic castration-resistant prostate cancer patient with

PSMA-negative/FDG-positive disease. *Eur J Nucl Med Mol Imaging.* 2019.

TABLE 1. Clinical characteristics and IgG4-RD involvements

No.	Age /sex	Biopsy site	Treatment	Serum IgG4 (mg/L)	Involvements of IgG4-RD
1	21/M	Pancreas	Prednisone, MMF	29300	Pituitary stalk, lacrimal gland, salivary gland, lung, pleura, pericardium, liver, gall bladder, pancreas, prostate, LN
2	58/M	Parotid	None	11300	Salivary gland, lung, pancreas, prostate, LN
3	52/M	Gall bladder	None	71700	Lacrimal gland, salivary gland, intrahepatic bile duct, pancreas, prostate, LN
4	56/M	Lacrimal gland	Prednisone	14600	Lacrimal gland, extraocular muscle, salivary gland, pleura, pancreas, periaortitis, peritoneum, LN
5	60/M	None	None	14400	Lacrimal gland, salivary gland, pancreas
6	59/F	Pancreas	None	11700	Lacrimal gland, salivary gland, pancreas, LN
7	24/F	None	None	3510	Retroperitoneal fibrosis
8	55/M	Pancreas	None	34100	Lacrimal gland, salivary gland, intrahepatic bile duct, liver, pancreas, prostate, LN
9	62/M	Lacrimal gland	None	27900	Lacrimal gland, salivary gland, nasal cavity, pleura, prostate, seminal vesicle, peritoneum, LN
10	63/M	None	None	1530	Retroperitoneal fibrosis, LN
11	17/M	Submandibular gland, pancreas	None	1380	Salivary gland, pancreas
12	42/F	Lung	Prednisone	355	Lacrimal gland, salivary gland, lung
13	55/M	None	None	21600	Lacrimal gland, salivary gland, lung, liver, pancreas, prostate, LN
14	57/M	None	None	33700	Lacrimal gland, salivary gland, lung, pleura, periaortitis, pancreas, prostate, seminal vesicle, LN
15	64/M	LN, kidney	None	28200	Nasal cavity, lung, pleura, intrahepatic bile duct, pancreas, periaortitis, kidney, prostate, LN
16	63/F	Submandibular gland, LN	None	47200	Lacrimal gland, salivary gland, lung, pancreas, LN
17	63/M	Submandibular gland	None	73400	Lacrimal gland, salivary gland, nasal cavity, lung, intrahepatic bile duct, pancreas, LN
18	40/M	None	None	6710	Pancreas, kidney, LN
19	51/M	Pancreas	Prednisone	34500	Salivary gland, pancreas, kidney
20	57/M	None	Prednisone, MMF	54400	Lacrimal gland, salivary gland, pancreas, kidney
21	59/F	None	None	3370	Retroperitoneal fibrosis, LN
22	55/M	None	None	3210	Salivary gland, pancreas
23	63/M	Pancreas	None	11900	Lacrimal gland, salivary gland, pancreas, prostate, LN
24	45/M	Pancreas	Prednisone, sirolimus, MMF	1730	Pancreas
25	50/F	Lung	Prednisone	580	Salivary gland, lung, pleura
26	47/M	Retroperitoneal mass	None	31100	Kidney and perirenal masses, peritoneum and retroperitoneal mass, seminal vesicle

MMF = mycophenolate mofetil; LN = lymph node

TABLE 2. Detectability of ^{68}Ga-FAPI and ^{18}F-FDG PET/CT in IgG4-RD

Involved organs	^{68}Ga-FAPI	^{18}F-FDG	*P* value
Lacrimal gland	14/14 (100%)	10/14 (71.4%)	0.125
Salivary gland	19/19 (100%)	18/19 (94.7%)	1.0
Lung/pleura	10/11 (90.9%)	10/11 (90.9%)	1.0
Pancreas	19/19 (100%)	11/19 (57.9%)	0.0078*
Bile duct/liver	6/6 (100%)	4/6 (66.7%)	0.480
Periaortitis/retroperitoneal fibrosis	7/7 (100%)	7/7 (100%)	1.0
Kidney	4/5 (80.0%)	4/5 (80.0%)	1.0
Prostate/seminal vesicle	10/10 (100%)	10/10 (100%)	1.0
Lymph node	0/16 (0%)	16/16 (100%)	<0.0001*

* The difference in the positive rate between ^{68}Ga-FAPI and ^{18}F-FDG is significant.

TABLE 3. SUVmax of IgG4-RD involvements in ^{68}Ga-FAPI and ^{18}F-FDG PET/CT

Involved organs	^{68}Ga-FAPI	^{18}F-FDG	*P* value
Lacrimal gland	4.81±1.64	5.64±4.10	0.433
Salivary gland	8.26±3.90	4.88±1.90	0.0008*
Lung/pleura	6.69±7.21	4.33±2.56	0.196
Pancreas	15.22±8.99	4.19±2.52	<0.0001*
Bile duct/liver	9.42±4.36	4.58±2.08	0.0081*
Periaortitis/retroperitoneal fibrosis	8.71±4.04	6.11±2.45	0.157
Kidney	9.44±6.67	4.02±1.58	0.106
Prostate/seminal vesicle	6.38±2.16	7.30±2.90	0.450
Lymph node	1.61±0.76	6.37±1.72	<0.0001*

* The difference of SUVmax between ^{68}Ga-FAPI and ^{18}F-FDG is significant.

	lacrimal gland	salivary gland	lung/pleura	pancreas	bile duct/liver	retroperitoneal fibrosis/ periaortitis	kidney	prostate/ seminal vesicle	lymph node
FAPI superior	6	11	2	16	5	1	1	0	0
equal	8	8	7	3	1	5	4	6	0
FDG superior	0	0	2	0	0	1	0	4	16
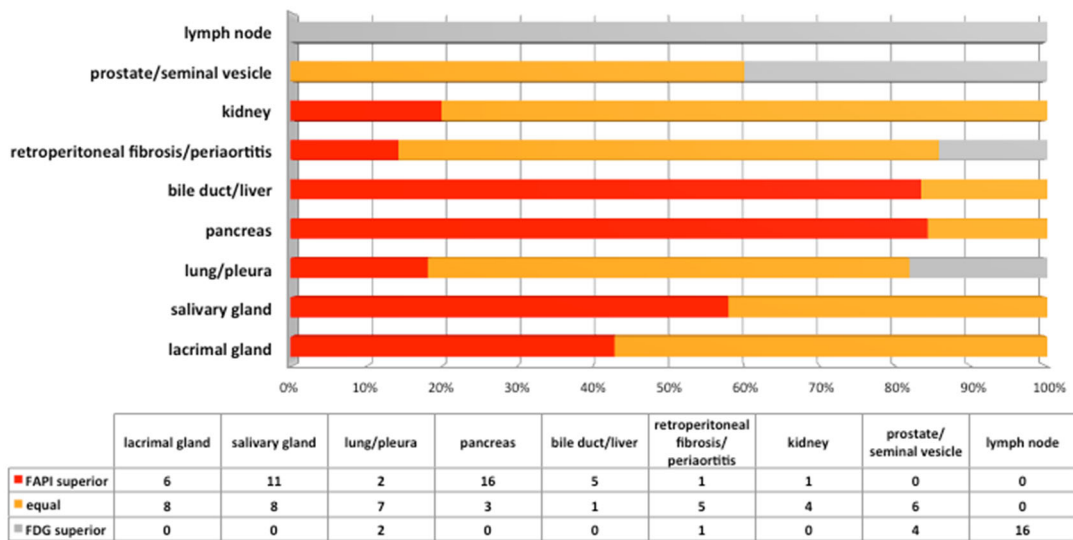
FIGURE 1. Visual comparison of organ involvements of IgG4-RD between ^{68}Ga-FAPI and ^{18}F-FDG PET/CT.
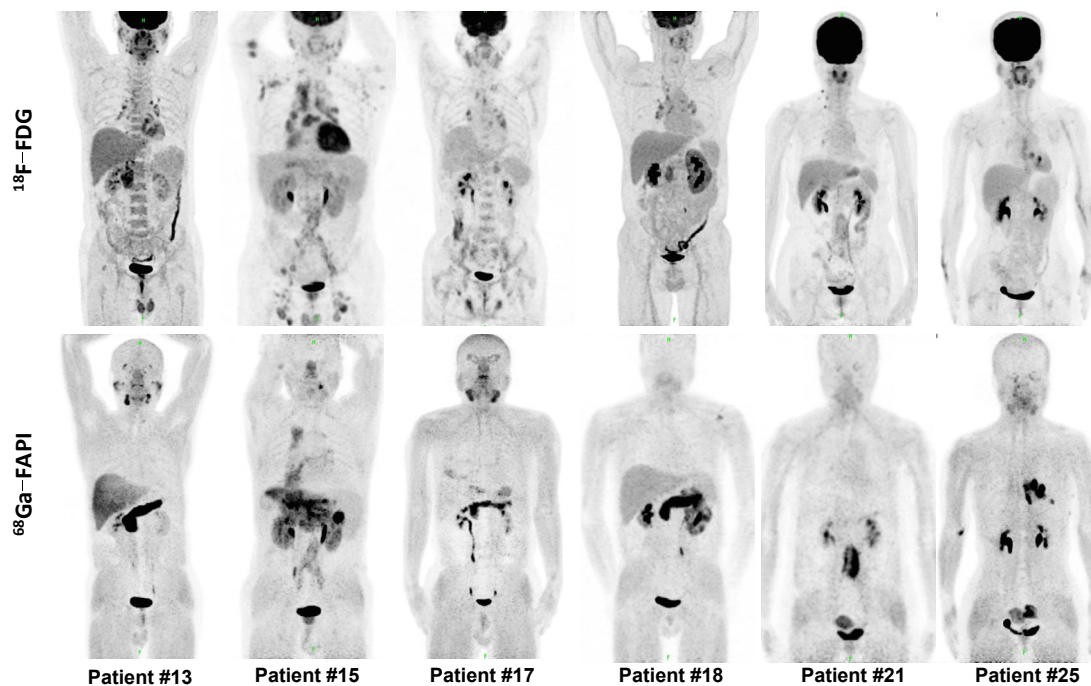
FIGURE 2. Intraindividual comparison of 6 patients with IgG4-RD undergoing ^{18}F-FDG and ^{68}Ga-FAPI PET/CT. Examples to show the superiority of ^{68}Ga-FAPI to ^{18}F-FDG in depicting involvements of IgG4-RD in the pancreas (patient #13, 15, 17, 18), bile duct/liver (patient #13, 15, 17), retroperitoneal fibrosis (patient #21), lung/pleura (patient #25), and salivary gland (patient #13, 17). Notice the hypermetabolic lymph nodes in ^{18}F-FDG PET/CT did not show uptake of ^{68}Ga-FAPI (patient #15, 17). Renal involvements (patient #15, 18) were both FDG- and FAPI-avid. There was also unspecific FAPI uptake in the uterus (patient #21, 25).

SUPPLEMENT TABLE 1. Diagnostic performance of dual tracer PET/CT in IgG4-RD

No.	Lacrimal gland		Salivary gland		Lung/pleura		Pancreas		Biliary duct /liver		Periaortitis /retroperitoneal fibrosis		Kidney		Prostate /seminal vesicle		Lymph node	
	FAPI	FDG	FAPI	FDG	FAPI	FDG	FAPI	FDG	FAPI	FDG	FAPI	FDG	FAPI	FDG	FAPI	FDG	FAPI	FDG
1	+	-	+	+	+	+	+	+	+	+	N	N	N	N	+	+	-	+
2	N	N	+	+	+	+	+	-	N	N	N	N	N	N	+	+	-	+
3	+	+	+	+	N	N	+	+	+	+	N	N	N	N	+	+	-	+
4	+*	+*	+	+	+	+	+	+	N	N	+	+	N	N	N	N	-	+
5	+	-	+	+	N	N	+	+	N	N	N	N	N	N	N	N	N	N
6	+	+	+	+	N	N	+	+	N	N	N	N	N	N	N	N	-	+
7	N	N	N	N	N	N	N	N	N	N	+	+	N	N	N	N	N	N
8	+	-	+	+	N	N	+	+	+	+	N	N	N	N	+	+	-	+
9	+	+	+	+	+	+	N	N	N	N	N	N	N	N	+	+	-	+
10	N	N	N	N	N	N	N	N	N	N	+	+	N	N	N	N	-	+
11	N	N	+	+	N	N	+	+	N	N	N	N	N	N	N	N	N	N
12	+	+	+	+	-	-	N	N	N	N	N	N	N	N	N	N	N	N
13	+	+	+	+	+	+	+	+	+	-	N	N	N	N	+	+	-	+
14	+	+	+	+	+	+	+	-	N	N	+	+	N	N	+	+	-	+
15	N	N	N	N	+	+	+	+	+	+	+	+	+	+	+	+	-	+
16	+	+	+	+	+	+	+	-	N	N	N	N	N	N	N	N	-	+

17	+	+	+	+	+	+	+	-	+	-	N	N	N	N	N	N	-	+
18	N	N	N	N	N	N	+	+	N	N	N	N	+	+	N	N	-	+
19	N	N	+	-	N	N	+	-	N	N	N	N	-	-	N	N	N	N
20	+	-	+	+	N	N	+	-	N	N	N	N	+	+	N	N	N	N
21	N	N	N	N	N	N	N	N	N	N	+	+	N	N	N	N	-	+
22	N	N	+	+	N	N	+	+	N	N	N	N	N	N	N	N	N	N
23	+	+	+	+	N	N	+	-	N	N	N	N	N	N	+	+	-	+
24	N	N	N	N	N	N	+	-	N	N	N	N	N	N	N	N	N	N
25	N	N	+	+	+	+	N	N	N	N	N	N	N	N	N	N	N	N
26	N	N	N	N	N	N	N	N	N	N	+	+	+	+	+	+	N	N

*Extraocular muscle was also involved.

Fibroblast activation protein targeted PET/CT with ^{68}Ga-FAPI for imaging IgG4-related disease: comparison to ^{18}F-FDG PET/CT

Yaping Luo, Qingqing Pan, Huaxia Yang, Linyi Peng, Wen Zhang and Fang Li

This article and updated information are available at:
http://jnm.snmjournals.org/content/early/2020/06/05/jnumed.120.244723

Information about reproducing figures, tables, or other portions of this article can be found online at:
http://jnm.snmjournals.org/site/misc/permission.xhtml

Information about subscriptions to JNM can be found at:
http://jnm.snmjournals.org/site/subscriptions/online.xhtml

JNM ahead of print articles have been peer reviewed and accepted for publication in *JNM*. They have not been copyedited, nor have they appeared in a print or online issue of the journal. Once the accepted manuscripts appear in the *JNM* ahead of print area, they will be prepared for print and online publication, which includes copyediting, typesetting, proofreading, and author review. This process may lead to differences between the accepted version of the manuscript and the final, published version.

SNMMI | SOCIETY OF NUCLEAR MEDICINE AND MOLECULAR IMAGING